



This article appeared in a journal published by Elsevier. The attached copy is furnished to the author for internal non-commercial research and education use, including for instruction at the authors institution and sharing with colleagues.

Other uses, including reproduction and distribution, or selling or licensing copies, or posting to personal, institutional or third party websites are prohibited.

In most cases authors are permitted to post their version of the article (e.g. in Word or Tex form) to their personal website or institutional repository. Authors requiring further information regarding Elsevier's archiving and manuscript policies are encouraged to visit:

<http://www.elsevier.com/copyright>



Contents lists available at ScienceDirect

Vision Research

journal homepage: www.elsevier.com/locate/visres

High-resolution BOLD fMRI measurements of local orientation-dependent contextual modulation show a mismatch between predicted V1 output and local BOLD response

Jennifer F. Schumacher^{a,*}, Cheryl A. Olman^b^a Department of Neuroscience, University of Minnesota, N-218 Elliott Hall, 75 East River Parkway, Minneapolis, MN 55455, USA^b Departments of Psychology and Radiology, University of Minnesota, N-218 Elliott Hall, 75 East River Parkway, Minneapolis, MN 55455, USA

ARTICLE INFO

Article history:

Received 27 June 2009

Received in revised form 1 January 2010

Keywords:

fMRI

Primary visual cortex (V1)

Surround suppression

Contrast

Psychophysics

ABSTRACT

The blood oxygenation level-dependent (BOLD) functional MRI response to suppressive neural activity has not been tested on a fine spatial scale. Using Gabor patches placed in the near periphery, we precisely localized individual regions of interest in primary visual cortex and measured the response at a range of contrasts in two different contexts: with parallel and with orthogonal flanking Gabor patches. Psychophysical measurements confirmed strong suppression of the target Gabor response when flanked by parallel Gabors. However, the BOLD response to the target with parallel flankers decreased as the target contrast increased, which contradicts psychophysical estimates of local neural activity.

Published by Elsevier Ltd.

1. Introduction

Because many interesting details of neural coding are found on a fine spatial scale, the high spatial resolutions achievable in fMRI are attractive to many neuroscientists. The first goal of the experiments reported here was to accurately localize and analyze the blood oxygenation level-dependent (BOLD) response to a specific spatial location in a visual scene. This precise localization should provide a better interpretation of the underlying neural activity. For example, our understanding of the neural processes associated with change blindness and many visual illusions would be improved by the ability to study responses to individual image features. Previous work has suggested that the spatial accuracy of GE BOLD is about 3.5 mm, based on the vascular point spread function (PSF) (Das & Gilbert, 1995; Engel, Glover, & Wandell, 1997; Ogawa et al., 1993; Parkes et al., 2005). For the neural response itself, smaller neural PSFs (2–3 mm) are expected based on the spatial extent of horizontal connections and dendritic arbor geometry (Amir, Harel, & Malach, 1993; Angelucci et al., 2002; Grinvald, Lieke, Frostig, & Hildesheim, 1994). Here we investigate whether the BOLD response to clusters of neural activity approximately 5 mm apart on the cortex can be distinguished reliably and whether suppression by parallel context is apparent in the BOLD signal.

* Corresponding author.

E-mail addresses: schum204@umn.edu (J.F. Schumacher), caolman@umn.edu (C.A. Olman).

Studying surround suppression with BOLD fMRI on a local scale will allow further insight into how humans view and parse visual scenes by studying how context modulates the response to individual features. Inhibition is a fundamental aspect of visual processing, playing a role in neural computations both between and within cortical areas of the brain. To investigate the BOLD response to local inhibition, we use surround suppression, which has been studied extensively (a selection pertinent to our research: Cavanaugh, Bair, & Movshon, 2002; Polat, Mizobe, Pettet, Kasamatsu, & Norcia, 1998; Zenger-Landolt & Koch, 2001) and is strong in the near periphery (1–4° eccentricity) (Petrov, Carandini, & McKee, 2005; Xing & Heeger, 2000). In both electrophysiological (Cavanaugh et al., 2002) and psychophysical (Zenger-Landolt & Koch, 2001) experiments, a stimulus with a parallel surround exhibits a suppressed neural response compared to the stimulus alone, and an orthogonal surround results in either weaker suppression or facilitation.

Literature reports on the BOLD response to neural suppression conflict, claiming either an increase or a decrease in the BOLD response during neural suppression. Several studies show a decrease in the BOLD response with neural inhibition (Chen, Silva, Yang, & Shen, 2005; Devor et al., 2007; Northoff et al., 2007; Shmuel, Augath, Oeltermann, & Logothetis, 2006; Zenger-Landolt & Heeger, 2003). However, there is also work that predicts an increase in the BOLD response with neural inhibition (Ackermann, Finch, & Babb, 1984; Cauli et al., 2004; Lauritzen, 2001; Nie & Wong-Riley, 1995; Pelled et al., 2009). When responses are measured over a

large cortical area, a comparison of visual psychophysics and BOLD fMRI finds that neural suppression induces a decrease in the BOLD response (Pihlaja, Henriksson, James, & Vanni, 2008; Zenger-Landolt & Heeger, 2003). The experiments described here use a flanking inhibition paradigm with single target Gabor patches to test whether the BOLD response decreases when a parallel surround suppresses neural activity. Our data show that the localized BOLD response does not match the inferred local neural activity, indicating that the BOLD response can not always be simply predicted by the response in neurons tuned to the presented stimulus and suggesting that more complex models of neurohemodynamic coupling may be required to interpret BOLD responses of individual image features in a complex context.

2. Materials and methods

2.1. Subjects

We performed three separate experiments, and each experiment's data were collected from three human subjects from a pool of five subjects (four female, age 21–36, mean age 27.6) with normal or corrected to normal vision. The experimental protocols conformed to safety guidelines for MRI research and were approved by the Institutional Review Board at the University of Minnesota. Subjects provided written informed consent before participating in the experiments.

2.2. Visual stimuli

The targets-alone stimuli for the first experiment (Fig. 1A, top) consisted of four Gabor patches located in each of the four visual quadrants at 3° eccentricity. Each Gabor patch consisted of a 3 cycles-per-degree (cpd) sinusoidal grating modulated by a Gaussian envelope with full width at half-maximum of 0.6° ($\sigma = 0.25^\circ$). The contrast response stimuli (second experiment) were the same as the targets-alone condition in the target and flankers experiment; however the orientation of the sinusoidal grating was randomized for each Gabor patch during each interval to avoid adaptation.

In the first experiment, (the main experiment, measuring the BOLD response to the target Gabors with parallel and orthogonal context), flanking Gabor patches were located on either side of the target Gabor with a center-to-center distance of 1° between target and flanker. Flankers were always presented at 50% contrast and were oriented either orthogonal to or parallel to the target Gabor. Stimuli for both the target and flankers experiment and the contrast response to targets-alone stimuli were displayed on a NEC 2180UX LCD monitor, subtending 8° × 11° of visual angle at a viewing distance of 200 cm.

The annulus stimuli (third experiment) were modeled after the center/surround stimulus used in Zenger-Landolt & Heeger, 2003. The central annulus extended from 2° to 4° eccentricity and the surround extended from 0.5° to 2° and from 4° to 8° eccentricity. Both the central annulus and the surround consisted of a 2 cpd sinusoidally modulated luminance grating. The orientation of the gratings changed after each trial and the gratings were contrast reversing at a rate of 4 Hz to avoid adaptation. The surround was always presented at 100% contrast and was oriented parallel to the central annulus. Stimuli were projected by a Sanyo (Sanyo North America Corporation, San Diego, CA, USA) projector with a custom zoom lens (NuView lens by Navitar, Rochester, NY, USA), housed outside the magnet room, onto a screen placed in the back of the magnet, and viewed from a mirror over the subjects' eyes.

All stimuli were presented on a mean gray background. Stimuli were generated and presented with Matlab (Mathworks, Inc.,

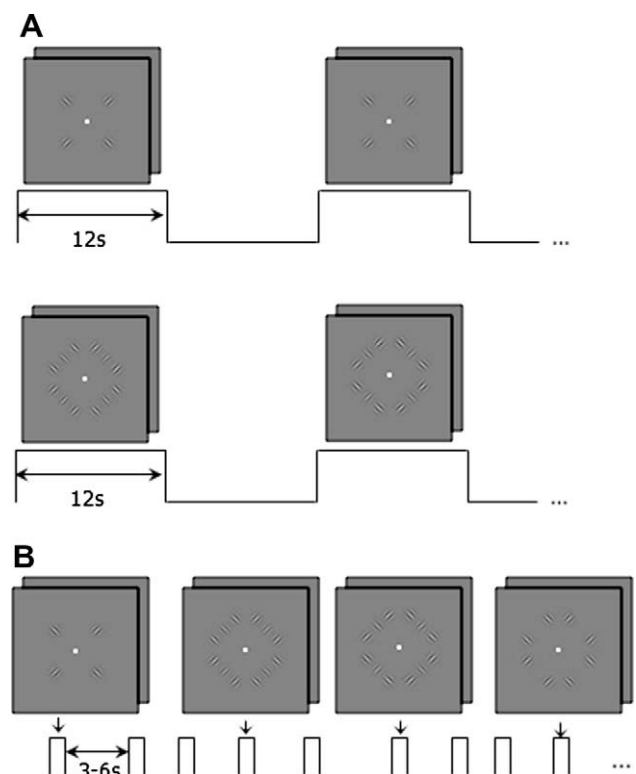


Fig. 1. Stimuli used to study contextual modulation in V1. (A) Targets-alone (top) and targets-with-flankers (bottom) block localizer scans. Stimuli were presented in the same 2IFC paradigm, 6 trials per 12 s block. During “blank” blocks subjects performed a 2IFC contrast detection task with a 0% target pedestal contrast. Ten and one half cycles were completed per scan. (B) Stimuli for event-related scans: targets with parallel flankers (target contrast was 8%, 16%, or 32%), targets with orthogonal flankers (again, target contrast was 8%, 16%, or 32%), targets-alone (32% contrast on all trials), and flankers-alone (50% contrast). Stimuli were presented in a two-interval forced choice (2IFC) paradigm (stimulus duration: 250 ms, inter-stimulus interval (ISI): 500 ms) Inter-trial interval was 3, 4.5 or 6 s (randomly selected for each trial).

Natick, MA) and Psychtoolbox (Brainard, 1997; Pelli, 1997). Macintosh G4 computers with OS X served as the processors for the psychophysics and fMRI systems.

2.3. Psychophysics

Contrast response functions for three stimulus configurations (targets-alone, targets with parallel flankers, and targets with orthogonal flankers) were estimated from contrast discrimination thresholds. For these psychophysical measurements, a Bits++ digital video processor (Cambridge Research Systems Ltd., UK) was used with the LCD monitor to provide 14-bit brightness resolution. Eight pedestal contrasts were employed for the target Gabor patches: 0%, 1%, 2%, 4%, 8%, 16%, 32%, and 64%. On each trial, all four targets appeared. On one of the two intervals in the trial, one of the four targets was incremented in contrast. The stimulus was presented for 250 ms in each interval, with a 500 ms blank inter-stimulus interval. Subjects maintained fixation on a white square at the center of the stimulus set while indicating the interval (1 or 2) in which one of the target Gabors increased in contrast; feedback for the task was given by a green (‘correct’) or red (‘incorrect’) color at fixation after each response. A 3-down 1-up staircase was used to control the contrast increment on each trial; this staircase converged at a performance level of 79% correct, which was used as the threshold estimate for each pedestal contrast for each stimulus condition. Five threshold estimates (5 runs of 40 trials) at each of

the eight contrast levels for each condition (targets-alone, targets with orthogonal flankers, and targets with parallel flankers) were completed per subject.

Threshold versus contrast (TvC) curves for each condition and each stimulus type were fit (using Matlab's `lsqcurvefit` function) with a variant of the Naka–Rushton formula (Eqs. (1) and (2), see (Zenger-Landolt & Heeger, 2003)). The extra parameters in this fit allow for the fact that flankers suppress the target response when target contrast is lower than flanker contrast, but flankers become consistently facilitative when the target contrast is greater than the flankers. The inferred contrast response function for each stimulus configuration was the integral of this function. Parameters used to fit the data from Subject 2 (Fig. 2, middle column) are shown in Table 1.

$$r(x) = ax^p / (x^{p-q} + b^{p-q}) \tag{1}$$

$$x(c) = dc + ec^f \tag{2}$$

2.4. fMRI Experiments

The target and flankers BOLD fMRI experiment (Experiment 1) was completed on a Siemens Trio 3T system (Siemens, Erlangen, Germany) at the Center for Magnetic Resonance Research at the University of Minnesota. The scanner was equipped with Sonata gradients (maximum amplitude: 40 mT/m; slew rate: 200 T/m/s). An eight-channel RF head-coil was used to acquire gradient echo (GE) EPI images. Field of view was 192 mm × 144 mm with a matrix size of 128 × 96 (6/8 partial Fourier acquisition) for a nominal

Table 1

Parameter values implemented to fit the TvC curves with Eqs. (1) and (2) for psychophysics results for Subject 2 presented in Fig. 2 (middle column).

	<i>a</i>	<i>b</i>	<i>d</i>	<i>e</i>	<i>f</i>	<i>p</i>	<i>q</i>
Target	35	109	84	0.20	2.6	1.7	0.32
Target with parallel flankers	47	147	112	0.22	3.5	1.6	0.19
Target with orthogonal flankers	46	178	148	0.36	2.7	1.8	0.25

inplane resolution of 1.5 mm isotropic. Slice thickness was 1.5 mm, volume repetition time (TR) was 1.5 s and echo time (TE) was 30 ms. Seventeen slices were prescribed perpendicular to the calcarine sulcus in an oblique coronal orientation and covered early visual areas.

For the target and flankers experiment, each subject completed four scanning sessions on separate days. One session was for standard retinotopic mapping and acquisition of an MP-RAGE anatomy (1 mm isotropic resolution). The remaining three sessions each included three target localizer scans (block design, Fig. 1A top), three target with flankers (superset) localizer scans (block design, Fig. 1A bottom), and three event-related scans (Fig. 1B).

Targets were presented at 32% contrast in the block localizer scans. For the targets-alone localizer, subjects performed a contrast discrimination task as in the psychophysical measurements. During “on” blocks the target pedestal contrast was 32%; during “off” blocks the target pedestal contrast was 0%. On and off blocks each lasted 12 s; 11 on blocks alternated with 10 off blocks during each scan, and the first on block was discarded before analysis. The superset localizer scans had the same block design, but subjects per-

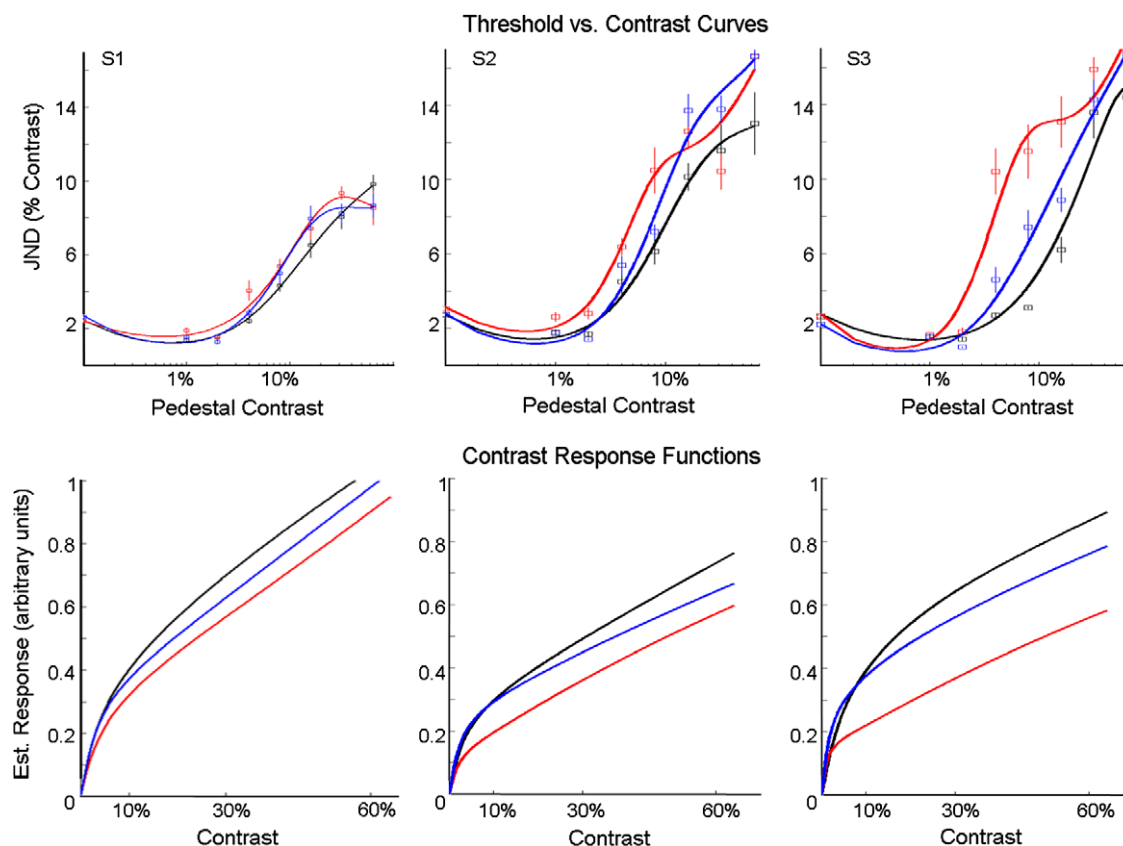


Fig. 2. Psychophysical quantification of suppression of target Gabor responses by flanking Gabor patches. The top row has threshold versus contrast plots (red: parallel flankers, blue: orthogonal flankers, black: targets-alone) while the bottom row shows inferred contrast response functions (calculated after fitting threshold versus contrast data with a variant of the Naka–Rushton formula, Eqs. (1) and (2)). Each column contains the result from a single subject. High contrast discrimination thresholds for the targets with parallel and orthogonal flankers translated to a low inferred neural response in the contrast response function (CRF) compared to the targets-alone configuration for all three subjects. Psychophysical measurements predict parallel flankers will suppress neural response to target Gabors 20–50% when the targets are at 16% contrast.

formed a contrast-matching task during the “on” blocks. Targets with orthogonal flankers were presented in one of the two intervals, and targets with parallel flankers were presented in the other. Subjects indicated the interval (1 or 2) in which the targets appeared to have higher contrast. Target contrast was adjusted on a staircase throughout the scan, converging at a contrast at which the targets with parallel flankers appeared to have the same contrast as with orthogonal flankers. On average, subjects required a 10% contrast increment before reporting matched perceived contrast for the two conditions; this approximately matched estimated contrast response functions from the psychophysical sessions. During the “off” blocks, subjects were engaged in a detection task for the targets-alone stimuli (all four were incremented together, as in the “on” blocks).

The event-related scans measured the BOLD response to eight stimulus conditions: targets-alone, flankers-alone, and six targets-with-flankers conditions. In the targets-alone condition, targets were presented with 32% contrast. In the flankers-alone condition, orthogonal flankers were used on half of the trials and parallel flankers on the rest. For the remaining six conditions, targets were presented at three contrast levels (8%, 16%, and 32%) with either parallel or orthogonal flankers. Flankers were always presented at 50% contrast. In the event-related scans, stimuli were presented with the same timing as in the psychophysical measurements and subjects were engaged in the same two-interval forced choice contrast discrimination task as in the psychophysics. Pairs of stimuli were presented with an inter-trial interval of 3, 4.5 or 6 s (inter-trial interval was randomly selected and uniformly distributed). Separate adaptive staircases were used to equate task demands between conditions; the flankers-alone conditions used a contrast detection task with 0% pedestal contrast targets. There were a total of 88 trials per scan (11 of each stimulus type), for a total of 33 presentations of each stimulus type on each day. Subjects viewed the stimuli via a mirror mounted on the head-coil; behavioral responses were collected using a fiber-optic button box (Current Designs, Philadelphia, PA).

The contrast response and annulus BOLD fMRI experiments (Experiments 2 and 3) were completed on the same magnet after it had been upgraded to a Siemens TIM Trio 3T system (Siemens, Erlangen, Germany) with Avanto gradients (maximum amplitude: 45 mT/m, slew rate: 200 T/m/s). A 12-channel RF receive-only head-coil was used to acquire the GE EPI images with a TR of 1.5 s and TE of 30 s. For the contrast response data (Experiment 2), the field of view was 256 mm × 256 mm with a matrix size of 128 × 128 for a nominal inplane resolution of 2 mm isotropic. Eighteen slices (2 mm slice thickness) were aligned perpendicular to the calcarine sulcus in an oblique coronal orientation covering early visual areas. For the annulus experiment (Experiment 3), the field of view was 192 mm × 192 mm with a matrix size of 64 × 64 for a nominal inplane resolution of 3 mm isotropic. Twenty-five slices (3 mm slice thickness) were aligned perpendicular to the calcarine sulcus in an oblique coronal orientation covering early visual areas.

For the contrast response experiment, two subjects participated in three scanning sessions each and the third subject participated in one scanning session. Each scanning session involved at least four functional localizers and three event-related scans. (The first two subjects participated in three scanning sessions because each session included eight additional block-design scans to estimate the contrast response function, and therefore only three or four event-related scans. The third subject participated in a scanning session with only four block-design localizers and six event-related scans.) Anatomical and retinotopic information were used from a previous scanning session. The contrast response scans were similar to the event-related target and flanker experiment, except the only stimulus was targets-alone, presented at 8%, 16%, and 32%

pedestal contrast. There were 15 trials of each contrast level per scan, for a total of at least 75 trials per scanning session. Block-design functional localizers, similar to Experiment 1, were used to define the target-alone ROIs, except with only eight “on” blocks and seven “off” blocks (each block lasting 12 s) per scan.

For the annulus experiment, each subject participated in one scanning session, which involved at least two central annulus localizer scans (differential block design) and at least six event-related scans (at least four scans with-surrounds and at least two scans without-surrounds). Anatomical and retinotopic information were used from a previous scanning session.

In the differential block localizer scans, the central annulus and the surround were presented at 100% contrast with a 50% duty cycle (0.75 s of 4 Hz contrast-reversing grating interleaved with 0.75 s of mean gray screen with a persistent fixation mark and black outline defining the annulus region divided into eight equal subregions). Subjects performed a contrast discrimination (central-annulus-alone blocks) or contrast detection (surround-alone blocks) task in which the contrast of one of the eight segments of the central annulus decreased (discrimination task) or increased (detection task) from the pedestal contrast on half of the trials. On and off blocks each lasted 12 s; 11 on blocks alternated with 10 off blocks during each scan, and the first on block was discarded before analysis.

Two different event-related scans were used to measure the BOLD response to the center annulus with and without-surrounds. The experiment design was modeled after Zenger-Landolt and Heeger (2003), but adapted to an event-related paradigm with the same stimulus presentation timing as the targets and flankers experiment. In the with-surrounds scan, the surround annuli were presented at a 50% duty cycle throughout the entire scan (present for 0.75 s, every 1.5 s). This design ensures that the measured hemodynamic response reflects the BOLD response to the center annulus itself, and is robust against hemodynamic suppression effects that may result from the extended surround grating. Three stimulus conditions were measured in the with-surrounds scans: 10%, 20%, and 40% contrast annulus with parallel surrounds. Surrounds were always 100% contrast. In the without-surrounds scans, two conditions were measured: the center annulus alone (40% contrast) and surround-alone (100% contrast). In all event-related scans, the stimuli were presented for 0.75 s with an inter-trial interval of 3, 4.5 or 6 s (inter-trial interval was randomly selected and uniformly distributed). A contrast discrimination task was used in which one of the eight segments of the central annulus decreased in contrast during half of the trials, except during the surround-only condition, in which a contrast detection task was employed since the central annulus was at 0% pedestal contrast. The fixation mark provided correct or incorrect feedback for the task by turning green or red, respectively. There were a total of 60 trials for each stimulus condition per scanning session (four with-surrounds scans with 15 presentations of each stimulus type, and two without-surrounds scans with 30 presentations of each stimulus type).

2.5. fMRI Data analysis

Preprocessing of functional data, which included motion compensation, high-pass filtering, and alignment of functional data to the reference anatomy (Nestares & Heeger, 2000), was accomplished with custom Matlab code. Fieldmap-based distortion compensation for the EPI images was completed with FSL (Smith et al., 2004). For the reference anatomy, gray/white matter segmentation, cortical surface reconstruction and surface inflation and flattening were completed in SurfRelax (Larsson, 2001). Standard retinotopic mapping (DeYoe et al., 1996; Engel et al., 1997; Sereno et al., 1995) using rotating wedges and expanding rings was used

to identify V1 and an iso-eccentricity band centered at 3° of visual angle from the fovea. Boundaries for visual areas were translated to the reference anatomy, and from there to the functional data, to restrict where ROIs would be defined for further analysis.

For each target and flankers and contrast response scanning session (Experiments 1 and 2), ROIs were selected based on retinotopic location and functional localizers. Voxels within the pre-selected 3° eccentricity band in V1 with coherence exceeding 0.15 (Bandettini, Jesmanowicz, Wong, & Hyde, 1993; Engel et al., 1997) during the appropriate localizer (target or superset) were initially defined in the flat cortical representation and then translated to the in-plane anatomy for selection of only contiguous voxels. A phase window from about $\pi-1.6\pi$ was used to select BOLD responses that were positive when the stimulus was present. Similarly, for the contrast response data, voxels within this same retinotopic area but exceeding a coherence of 0.3 during the functional localizers were used for the ROI. (A larger coherence threshold was used for Experiment 2 because more functional localizer scans were available per subject.)

A general linear model (GLM) was used to analyze the event-related data. Custom Matlab code estimated the amplitude of the BOLD response for 12 time points (18 s) after the stimulus onset to avoid making assumptions about the shape of the hemodynamic response function (HRF). Multiple scans from a given scanning session were concatenated in time and a single HRF was estimated for each stimulus type for each scanning session. Hemodynamic responses were characterized either by the peak amplitude of the response (4.5 s after the stimulus onset) or by the amplitude of a difference-of-gamma functions HRF model fit to the data. Both methods produced identical results for the overall pattern of BOLD responses. For the target and flankers experiment, BOLD response amplitudes were calculated for individual subjects (3) on separate days (3), and then averaged (for $n = 9$).

The contrast response data were motion compensated with FSL's MCFLIRT function (Jenkinson, Bannister, Brady, & Smith, 2002), but otherwise used the same preprocessing steps and GLM analysis as the target and flankers experiment. Fifteen percent of the highest variance voxels were removed from the ROI to eliminate voxels dominated by large vessels (Olman, Inati, & Heeger, 2007) and thereby minimized localization errors. The contrast response hemodynamic response estimates were averaged across scanning sessions for each subject: three sessions (20 total event-related scans for the first subject), three sessions (12 total event-related scans) for the second, and one session (nine event-related scans) for the third.

The same preprocessing and GLM methods were used for the annulus fMRI experiment, except distortion compensation was not used. ROIs were defined based on retinotopic information and the differential block localizers. Voxels within the pre-selected 2–4° eccentricity band in V1 with coherence exceeding 0.3 (Bandettini et al., 1993; Engel et al., 1997) during the functional localizer were initially defined in the flat cortical representation and then translated to the inplane anatomy for selection of only contiguous voxels. A separate ROI was created for each hemisphere for each subject, totaling $n = 6$ for the final analysis. Fifteen percent of the highest variance voxels were removed from the ROI to eliminate voxels dominated by large vessels. The difference-of-gamma HRF fits were determined per hemisphere and then peak amplitudes were averaged.

2.6. Expected size of cortical representation of stimuli

As a rough estimate of the size of the cortical territory representing each individual Gabor patch, the functional form for human cortical magnification estimated by Engel et al. (1997) was used:

$$E = e^{0.063 \cdot (x+36.54)}, \text{ or } x = (\ln(E)/0.063) - 36.54$$

where x is cortical distance in millimeters (from the cortical location where 10° eccentricity is represented), and E is eccentricity. A Gabor patch that is 0.6° wide (FWHM) at 3° eccentricity therefore extends from -21 to -17.5 mm on the cortex (in a radial direction). Assuming roughly symmetric cortical representation and constant cortical thickness, the neural representation of the Gabor is estimated to occupy a cylindrical cortical territory described by a circle with radius 3.5 mm, projecting through the depth of the gray matter (approximated as 3 mm on average, for a total cortical volume of 115 mm^3 , or 34 1.5 mm isotropic voxels). Following the same logic, the central annulus for Experiment 3 occupies a band of cortex with a width of 11 mm, projecting through the depth of the gray matter.

3. Results

3.1. Psychophysics

To confirm suppression of the neural response to target stimuli in the presence of local parallel context, we measured contrast discrimination thresholds as a function of target pedestal contrast for three stimulus conditions: targets-alone, targets with orthogonal flankers and targets with parallel flankers (Fig. 1). The flanking Gabor patches were always presented at 50% contrast, for both the psychophysical measurements and for the subsequent BOLD experiment. In the psychophysical measurements, we found suppression for both the orthogonal and parallel conditions compared to the targets-alone responses, with more suppression for the parallel configuration (Fig. 2), consistent with (Zenger-Landolt & Koch, 2001). Behavioral data from the fMRI experiments revealed a similar pattern of responses, albeit with smaller thresholds, most likely because there were only 11 trials per scan and the contrast increment started low (data not shown).

3.2. Localization of specific spatial locations

To localize specific cortical regions of interest (ROIs), two separate arrangements of Gabor patches were used as visual stimuli (Fig. 1A): a targets-alone stimulus and a targets-with-flankers-stimulus. A target ROI set consists of four sub-ROIs representing the four target locations. A superset ROI set consists of the four regions of cortex responding to the four sets of targets and flankers (both orientations of flankers were used for the localizer). Each stimulus (targets-alone and targets-with-flankers) was used in a separate block design localizer as described in the Methods section.

Results from the block localizer scans are summarized in Fig. 3. The definition of both the target and the superset (targets-with-flankers) ROIs is shown for a representative subject (Fig. 3A). The average response of each target component ROI (single Gabor patch) was a volume of 28 (1.5 mm isotropic) voxels; the average volume of each superset component ROI (three Gabor patches) was 81 voxels. Predicted ROI volumes based on typical cortical magnification factors in humans were 34 voxels for each component of the target ROIs, and 102 voxels for each component of the superset ROIs.

The repeatability of localization of a particular spatial location in the visual field over three scanning sessions is shown for a single subject in Fig. 3B. ROIs from each day (session) were translated to the volume anatomy, and each session's target ROI is outlined in a different color. Some errors in ROI definition and/or alignment are obvious – for example, the Day 1 ROI (blue outline) contains a significant amount of white matter. This is likely due to an imperfect registration between the functional and anatomical data for that data set. To illustrate variability across the entire experiment, the volumes and centers of mass for each target ROI for each day in

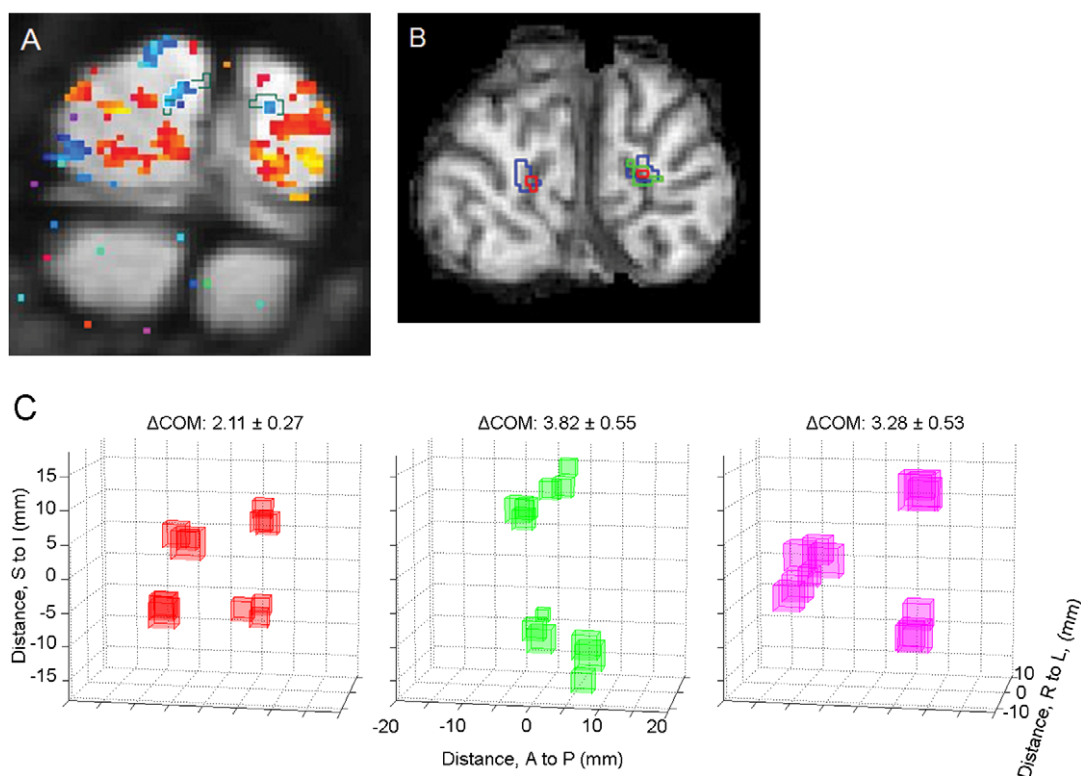


Fig. 3. ROI localization. (A) Functional data from target block localizers (averaged data from three days, a total of nine target-alone localizer scans), for one subject (S3), overlaid on mean functional image (color map: blue indicates in-phase with stimulus presentation, red indicates out of phase with stimulus presentation). Target ROI is indicated by white outline, superset ROI (identified by a different set of functional data) is indicated by dark green outline. Two of four sub-ROIs are visible in this particular slice; the other two sub-ROIs are located in different slices. (B) Target ROIs from three different days for the same subject, translated to the reference anatomy (1 mm isotropic resolution) and shown on a single coronal slice (Blue: Day 1, Green: Day 2, Red: Day 3). (C) Three-dimensional plots of all target ROI locations for all subjects for three days. For each subject, each sub-ROI is represented by a cube centered at the calculated center of mass (COM). The volume of the cube indicates the volume of the sub-ROI. Indicated above each plot is the average pairwise 3D Euclidian distance between sub-ROI COMs from the three different days ($n = 12$ comparisons, three for each of four locations, for each subject).

each subject are shown in Fig. 3C. We quantified the precision of our spatial localization by averaging the three-dimensional cortical distances between each center of mass for each component ROI over the three days in the volume anatomy. The average Euclidean distances and standard error of the mean between individual day target ROI centers of mass were $2.11 \text{ mm} \pm 0.27$, $3.82 \text{ mm} \pm 0.55$, and $3.28 \text{ mm} \pm 0.53$ for the three subjects.

3.3. BOLD response to contextual modulation

Three scans with an event-related design were also completed during each scanning session for Experiment 1, using a total of eight stimuli: targets-alone, targets with parallel flankers for three different target contrasts (8%, 16%, 32%), targets with orthogonal flankers for three different target contrasts (8%, 16%, 32%), and flankers-alone (in the orthogonal configuration on half of the trials, and in the parallel configuration on the other half). Flankers were always presented at 50% contrast. Using ROIs determined from both the target and the superset block localizers, HRFs were estimated for 12 time points (18 s) following stimulus onset.

Fig. 4 shows HRFs in the target ROI for all conditions for one subject's average BOLD response over three scanning sessions. Even with blurring due only to motion compensation for a single day, the BOLD response in the target ROI contains a strong contribution from the flankers – the flankers-alone response (green line, Fig. 4A) is not only apparent in the target ROI, but is also among the largest in amplitude (even though the target stimulus is not present). This result might be predicted from blurring of the hemodynamic and/or neural responses. As a further indication of significant blurring

in the hemodynamic response, the pattern of results in the target ROI (Fig. 4D, described below) was the same as the pattern of results in the superset ROI (Fig. 4E).

Significant and opposite patterns were found for the orthogonal and parallel conditions as a function of target contrast. For the orthogonal condition, the peak BOLD response increased as the target contrast increased (Fig. 4B and D). For the parallel flanker condition, the amplitude of the BOLD response decreased as the target contrast increased (Fig. 4C and D). The interaction between the orthogonal and parallel conditions was significant ($F_{2,48} = 3.41$, $p = 0.041$, two-way ANOVA). The superset ROI also had a significant result for this comparison ($F_{2,48} = 5.4$, $p = 0.008$, two-way ANOVA).

A decrease of the BOLD response with increasing target contrast is not expected – the target response is expected to be suppressed but increasing with contrast – however this pattern might be explained if (1) the BOLD response represents the sum of the target and flanker responses and (2) the response to the flankers is increasingly suppressed by the increasing target contrast. To test for this possibility, two of the subjects participated in a psychophysical experiment in which contrast discrimination thresholds were measured for the parallel flanking Gabors while the target contrast was varied. (Aside from the change in response target, stimuli and methods were identical to the psychophysical measurements of contrast discrimination thresholds for the target Gabors.) We measured discrimination thresholds for the parallel and orthogonal flankers with target contrast at 8%, 16% and 32% while the flankers' pedestal contrast was always 50%. As shown in Fig. 5, discrimination threshold decreased with increasing target contrast for both subjects. The logic generally used to link discrimination

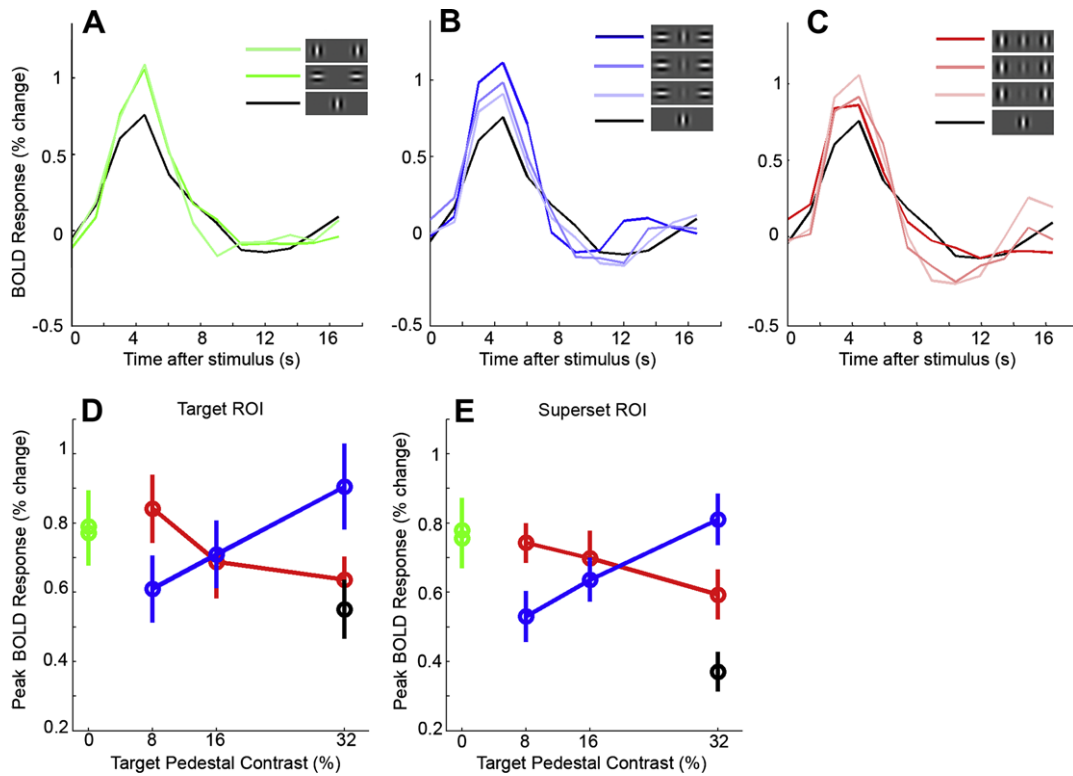


Fig. 4. Estimated BOLD fMRI responses in target ROI. (A–C) BOLD fMRI responses from one subject (S1), averaged over three scanning sessions. Target-alone condition is shown in black. (A) In the target ROI, the flanker-alone conditions (green lines) dominate even though no target Gabor patch is present. (B) Peak BOLD response increases with an increase in target contrast with orthogonal flankers. (C) Peak BOLD response decreases with an increase in target contrast with parallel flankers. (D–E) Response amplitude is estimated as the amplitude of a difference-of-gamma functions HRF model fit to the estimated HRFs, and error bars represent SEM. Significant interaction was found between the parallel and orthogonal conditions ($p < 0.05$, two-way ANOVA). (D) Summary of peak BOLD amplitude over all subjects, target ROIs (individual day data, $n = 9$). (E) Summary of peak BOLD amplitude over all subjects, superset ROIs (individual day data, $n = 9$). Similar patterns of results were obtained for both the target (D) and superset (E) ROIs.

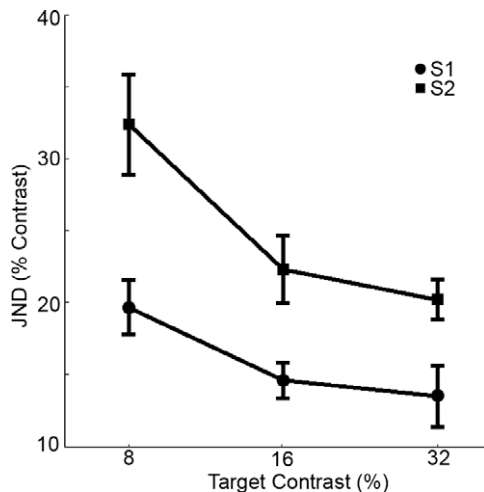


Fig. 5. Discrimination thresholds for parallel flankers with 50% pedestal contrast, under three different target contrast conditions (8%, 16%, 32% pedestal contrast); error bars are SEM ($n = 3$ threshold estimates per subject). Thresholds decreased with increasing target contrast for both subjects, which would not be the case if flanker response was suppressed by targets of higher contrast.

threshold measurements and neural (and BOLD) responses is that the threshold (just noticeable difference) is inversely related to the derivative of the neural response. The decreased threshold that we measured therefore indicates an increased slope of the neural response, which is consistent with facilitation rather than suppres-

sion. The model reported by Zenger-Landolt and Koch (2001) also predicts facilitation because the flanker contrast is higher than the target contrast. Therefore, the decrease of the BOLD response to the parallel configuration with increasing target contrast is not likely explained simply by dominance of the target ROI by flanker responses which are decreasing with increasing target contrast.

To ensure that the pattern of results in the target and flankers experiment was not a consequence of a general decoupling between the BOLD response and the neural response at a local scale, we measured the BOLD contrast response function to the target-alone stimulus (Fig. 6). In an event-related design, the target-alone stimulus was presented at 8%, 16%, and 32% pedestal contrast. We confirmed a linear BOLD contrast response for these target-alone pedestal contrast levels: the BOLD response increased with increasing contrast. Therefore, the high-resolution BOLD contrast response function behaves monotonically as it does in low resolution and larger stimulus experiments (e.g. Boynton, Demb, Glover, & Heeger, 1999).

Additionally, to ensure that the pattern of results in the target and flankers experiment was not an artifact of the fast-paced event-related design we measured orientation-dependent suppression of a large annulus with an orthogonal or parallel surround in the same event-related design (Fig. 7). We measured 21% suppression with parallel surrounds compared to the central-annulus-alone response and an increase in BOLD response with an increase in the central annulus with parallel surrounds pedestal contrast ($F_{2,15} = 3.53$, $p = 0.055$). The increasing contrast response in the parallel condition is what is expected for surround suppression and what we failed to find with the target and flankers experiment.

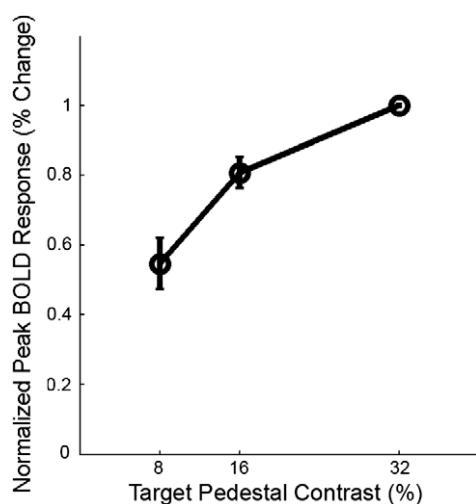


Fig. 6. BOLD response to target-alone Gabor patches at 8%, 16%, and 32% pedestal contrast. Contrast response functions for individual subjects were normalized by the response to the 32% contrast stimulus and averaged ($n = 3$, error bars indicate SEM).

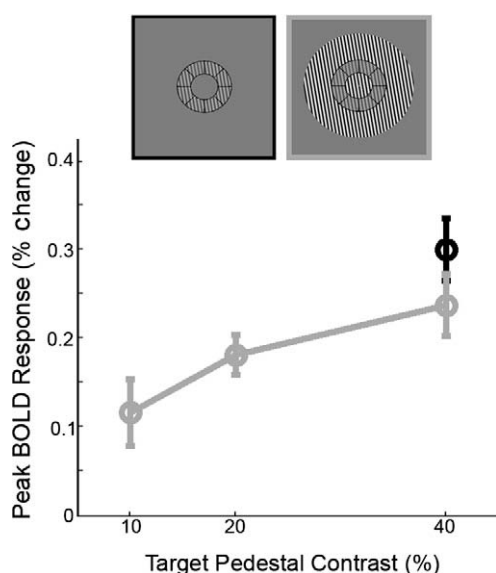


Fig. 7. Annulus experiment results: BOLD response to the center annulus increases with increasing contrast, in spite of the presence of the parallel surround. Error bars represent SEM ($n = 6$ hemispheres). The response to a 40% contrast center annulus is suppressed 21% by the presence of a parallel surround.

4. Discussion

By measuring localized BOLD responses to individual visual features with different local image contexts, we have found that responses to individual features can be localized with good precision across multiple days, but that even well-localized BOLD responses in V1 do not correlate with the suppression of V1 output that can be inferred by psychophysical measurements (and is reported in the electrophysiological literature). This finding can be interpreted in many ways, as discussed below. These interpretations range from mechanistic explanations (e.g., a dominance of inhibitory interneurons in regulating the hemodynamic response under our stimulus conditions) to the conclusion that the neural model we used to predict the BOLD data was insufficient (e.g., perhaps we failed to incorporate sufficiently complex neural responses in the model of the underlying neural activity). But the

basic value of the main experiment is that it defines at least one stimulus condition in which the models of neural response and neurohemodynamic coupling that successfully predict the BOLD response to large stimuli are insufficient for high-resolution measurements of small image features.

Psychophysical measurements of contrast discrimination thresholds were used to estimate the magnitude of neural activity in V1. In previous studies with a similar approach (Boynton, Demb, Glover, & Heeger, 1999; Zenger-Landolt & Heeger, 2003), the agreement between the magnitude of the BOLD response and the similarly estimated V1 neural response was good, even under conditions of strong suppression. Using center-surround stimuli composed of extended sine gratings, we did measure good agreement between BOLD and psychophysical estimates of surround suppression (Experiment 3), but in our main experiment this agreement between BOLD and estimated V1 response was not found. For a target Gabor at 3° eccentricity, psychophysical measurements indicate that parallel flanking Gabor patches suppress the V1 neural response (Cavanaugh, Bair, & Movshon, 2002, and our data, Fig. 2), but the suppressed neural response to the target Gabor patch nonetheless increases with increasing contrast. However, in a well-localized target ROI we measured the opposite pattern: adding suppressive flankers increased the response in the target ROI (which could be explained by blurring), and the BOLD response decreased with increasing target contrast in the parallel condition (a pattern that cannot be explained by blurring). The primary difference between the data reported here and previous studies showing good agreement between BOLD and neural response suppression (Boynton et al., 1999; Kastner et al., 2001; Pihlaja et al., 2008; Williams, Singh, & Smith, 2003; Zenger-Landolt & Heeger, 2003) is the spatial scale over which the responses were measured.

4.1. Spatial accuracy of this experiment

Just as blurring of the signal cannot explain our results because the pattern was basically independent of voxel selection, localization errors cannot explain our pattern of results. Nonetheless, it is important to understand the limits of our ability to localize individual image elements. We found that our day-to-day ROI localization was accurate to within several millimeters, which puts an upper limit on our localization errors. Some of these errors are due to errors in the alignment between the functional and anatomical data (e.g., the Day 1 outline appearing in the white matter when resampled from the functional data). Those alignment errors would not affect our conclusions because hemodynamic response functions were estimated from ROIs defined in the functional data space for individual subjects on individual days. Still, we could have small localization errors on individual days. The contrast-to-noise ratio in the target localizer data was relatively low (we used a low coherence threshold and a phase window to select voxels for the target ROIs in the targets and flankers experiment), which could potentially reduce the spatial accuracy in defining ROIs on individual days. However, there are two reasons to believe that localization errors did not create the pattern of results we measured. First, the volume of the target ROIs was well-matched to the expected ROI sizes based on typical cortical magnification functions in human visual cortex, and the locations were repeatable, so we are confident that there were no gross errors in ROI definition. Secondly, the pattern of results in the superset ROIs was almost identical to the pattern of results in the target ROIs, even though the superset ROIs were roughly three times the volume of the target ROIs. The similarity of the responses in the small and large volumes of cortex indicates that the particular pattern of results we observed was not a consequence of sampling or spatial localization. It is clear therefore that the pattern of results we

measured in the target and superset ROIs is a good characterization of the cortical BOLD response to the Gabor patches.

Like other studies investigating the spatial accuracy of the BOLD technique (Hulvershorn, Bloy, Lee, Leigh, & Elliott, 2005; Kriegeskorte, Cusack, & Bandettini, 2010; Olman et al., 2007), this study found that spatial accuracy is different in different regions of cortex: some of the sub-ROIs illustrated in Fig. 3 are reliably localized with precision better than 1 mm, while others show localization errors as large as several millimeters. Heterogeneity of spatial precision can be expected from both the geometry of the cortex and the geometry of the vasculature. Some target ROIs are near large veins (Subject 1, in particular, has one sub-ROI location near an obvious large vein in the calcarine sulcus), and their location can vary from experiment to experiment based on slight differences in the orientation of the subject's head in the scanner. Other target ROIs were simply on an outer surface of the cortex, rather than along a sulcus. Several of the sub-ROIs in Subject 2, the subject in which we found the lowest day-to-day repeatability in ROI location, were located on the posterior surface of the brain. Physiological noise and motion artifacts are more severe on the outer boundary of the cortex, where intensity changes in the image are abrupt and partial volume effects between gray matter and CSF make the voxels particularly sensitive to motion.

In spite of careful localization of target ROIs, we observed a strong response to the flanking Gabor patches (presented alone) in the target ROI, which suggests an inability to separate BOLD responses to visual features with centers separated by 1° of visual angle at 3° eccentricity (5 mm). It would be incorrect to attribute all of the spatial blurring of the signal to hemodynamic mechanisms. At least two additional sources of spatial blurring are present in the data. On the experimental side, the combined effects of subject motion and motion compensation, as well as the spatial registrations, cause blurring on a scale of a few millimeters. On the physiological side, neural activity is correlated over spatial scales much larger than a single neural column. Long-range horizontal connections in macaque monkeys can extend over a millimeter in either direction (Angelucci et al., 2002; Grinvald et al., 1994). Therefore, when investigating local contextual modulation, it is reasonable to expect that responses to neighboring stimuli will be confounded by even high-resolution BOLD measurements.

4.2. Other studies finding a mismatch between BOLD and V1 neural responses

Ours is not the only recent study to find a pattern of BOLD results that is not fully explained by psychophysics or neurophysiology. In studying interactions between collinear bar stimuli (a central bar with a flanking bar on each side), Kinoshita, Gilbert, and Das (2009) found that strong facilitation of the neural spike rate was accompanied by strong suppression in the optical imaging signal. This mismatch was measured only in the cortical area representing the central bar and not in the cortical area extending to include the flanking bars. The authors interpret this finding to suggest that the measured facilitation of spike rates is the result of complex interactions between excitatory and inhibitory inputs, which happen to result in a decreased hemodynamic response.

Another recent study has also reported an unexplained mismatch between the BOLD response to surround suppression and the estimated local neural response. Using center-surround stimuli and a range of stimulus sizes, Nurminen, Kilpeläinen, Laurinen, and Vanni (2009) measured perceptual summation and surround fields and found that they matched the size of neuronal summation and surround suppression reported in Cavanaugh, Bair, and Movshon (2002). The summation and surround field sizes measured with spin echo BOLD were, however, larger than the perceptual and neuronal summation fields. The measured response increased with

increasing stimulus size in the psychophysics, fMRI, and model data until it reached the size of the summation field; the response then decreased until asymptoting near the size of the surround field except in the case of the fMRI data, in which the response continued decreasing for all stimulus sizes.

4.3. Explanations based on neurohemodynamic coupling

Because the neurophysiological underpinnings of the BOLD response are not fully understood, one set of explanations for the discrepancy between our BOLD data and the predictions from psychophysics are based on possible differences in neurohemodynamic coupling on a local scale or when strong inhibition is present. We measured the contrast response for single Gabor patches at 3° eccentricity, finding a monotonically increasing function for contrasts used in the target and flankers experiment (Fig. 6). This is consistent with many other studies that have found a linear relationship between the BOLD response and the underlying neural activity and verifies that the discrepancy we found between the BOLD response and predicted local neural activity is not simply a consequence of the small size of the stimuli or the relatively high resolution of the experiment.

One untested explanation is that the dominant local suppression resulting from parallel flankers might interrupt the neurohemodynamic coupling by blocking the neural population responding to the target stimulus from recruiting more blood flow as contrast increases. This would result in decreased BOLD signal as a result of increased oxygen consumption without concomitant increase in blood flow. While it has been shown in cerebellar cortex that activation of inhibitory neurons alone does not increase blood flow (Li & Iadecola, 1994; Mathiesen, Caesar, Akgören, & Lauritzen, 1998, although see discussion of Pelled et al., 2009, below), it is not known how local blood flow responds to various combinations of excitatory and inhibitory neural activity.

As opposed to the potential under-recruitment of blood flow suggested above, a direct coupling between inhibitory neural activity and the hemodynamic response could also produce the result we observed. A recent paper by Pelled et al. (2009) shows that the positive BOLD response in ipsilateral somatosensory cortex following denervation of one paw in a rat may be attributable to increased inhibitory interneuron activity in the absence of excitatory activity. If local inhibitory neural activity plays a key role in driving the BOLD response, then the decrease in BOLD response with increasing target contrast could be explained by a reduction in the magnitude of inhibitory neural activity due to the reduction in local second-order contrast (Zenger-Landolt & Koch, 2001).

We have suggested two very different ways in which local neural computations with a strong inhibitory component could alter "normal" neurohemodynamic coupling. The energy demand of inhibitory neuronal activity and its subsequent effect on blood flow is unresolved (Attwell & Laughlin, 2001; Caesar, Thomsen, & Lauritzen, 2003; Cauli et al., 2004; Patel et al., 2005; Vaucher, Tong, Cholet, Lantin, & Hamel, 2000), and it may not be the case that arguments based on energetics are relevant because the energy demands of neural activity may not be directly related to the hemodynamic response (Devor et al., 2008; Sotero & Trujillo-Barreto, 2007). Nonetheless a growing body of literature suggests that, as the balance between excitation and inhibition is shifted in a local neural population, the BOLD response is not easily predicted.

4.4. Explanations based on an insufficient model for the neural activity

The above arguments also point to a second type of explanation for the pattern of results we measure: the BOLD response reflects local neural computations (Logothetis, 2003) and cannot be predicted from a univariate metric such as the output of neurons

tuned to the orientation of the target stimulus. Psychophysical techniques only estimate neural responses in one narrowly tuned neural population, while other local neural populations with different response properties also contribute to the BOLD response. For example, in our parallel flanker condition, second-order contrast (contrast between the target and flankers) decreases with increasing target contrast. A neural mechanism sensitive to this contrast (Larsson, Landy, & Heeger, 2006), whether originating in V1 or modulating V1 by feedback, would have a decreased response with increasing target contrast. A mechanism like this could also become significant only on a local scale, dominating only when the region of second-order contrast is large compared to the region of uniform contrast.

Similarly, the fact that adding a low-contrast target between orthogonal flankers decreased rather than increased the BOLD response (in both target and superset ROIs, Fig. 4D and E) might be explained by cross-orientation inhibition of neurons with receptive fields located so that they respond to both target and flanker Gabors. Given the complexity of neural responses in a single cubic millimeter of cortex, and the number of dimensions to which they are tuned, the models we use to predict V1 responses and interpret BOLD data are necessarily approximations – which may be valid in the case of extended sinusoidal gratings but fail for more localized stimuli.

A final possibility is that surround suppression might not originate in V1, and that we should not therefore expect the V1 BOLD response to match psychophysical measurements of suppression effects. Several researchers have suggested that feedback from higher visual areas is critical to contextual modulation (Hupe et al., 1998; Zipser, Lamme, & Schiller, 1996) and that the spatial scale of surround suppression is more consistent with the scale of feedback from higher visual areas than lateral connections within V1 (Angelucci et al., 2002; Schwabe, Obermayer, Angelucci, & Bressloff, 2006). However, this would not explain why BOLD measurements of suppression are consistent with psychophysics for large patches of sinusoidal gratings but not for local measurements of individual Gabor patches. Further work is therefore required to understand the source of neural suppression in early visual cortex as well as to develop appropriate models of neural response properties that can predict the modulation of the high-resolution BOLD response by local image context.

An alternative to developing a complete model of local neural activity to explain the BOLD response is to analyze the pattern of results simply to ask whether it contains information about particular stimulus attributes. Many recent studies using multi-voxel patterned activity (MVPA) and decoding approaches (Kamitani & Tong, 2005; Kay, Naselaris, Prenger, & Gallant, 2008) have circumvented the problems of spatial resolution and neural complexity by taking an indirect approach to measuring patterned activity in visual cortex. Rather than insisting on a one-to-one match between a voxel's response and the underlying neural activity, MVPA and decoding approaches simply ask whether the patterned BOLD activity clearly distinguishes between different stimuli or brain states. While such analyses do not elucidate the underlying neural code, they are valuable for determining aspects of the stimulus to which a given brain area is sensitive. The experiment we report here suggests that such indirect approaches may be the best option for studying patterned activity with 3T GE BOLD, at least for distinguishing responses to stimuli whose neural representations lie within several millimeters of each other.

5. Summary

These experiments have shown (i) successful localization of a particular spatial location over days in subjects, (ii) an inability

to separate BOLD responses to neighboring visual features separated by ~5 mm on cortex, and (iii) that, for the specific case of single Gabor patches flanked by parallel or orthogonal Gabors, high-resolution BOLD responses are not reliably correlated with V1 output predicted by psychophysical measurements. The response pattern we observed (decreasing BOLD response with increasing target contrast when flankers are parallel) could be explained by several factors, such as a strong effect of inhibitory interneurons in driving the BOLD response or a strong contribution from neurons other than the subset of the population that encode the target stimulus and serve the contrast discrimination task. Further work is necessary to determine how the neural model or the neurohemodynamic coupling model (or both) must be elaborated to treat sufficiently the case of local contextual modulation in primary visual cortex.

Acknowledgments

We thank S. Engel, J. Hegdé, D. Kersten, L. Holm, S. Thompson and two anonymous reviewers for their useful comments. Also thanks to Ari Holloway-Nahum for assistance with preliminary versions of the main experiment. The following funding sources supported this research: NIH-NPCS Graduate Student Training Fellowship, MIND Foundation, BTRR P41 RR008079, P30 NS057091 and NIH R01 EY015261.

References

- Ackermann, R. F., Finch, D. M., & Babb, T. L. (1984). Increased glucose metabolism during long-duration recurrent inhibition of hippocampal pyramidal cells. *Journal of Neuroscience*, 4(1), 251–264.
- Amir, Y., Harel, M., & Malach, R. (1993). Cortical hierarchy reflected in the organization of intrinsic connections in macaque monkey visual cortex. *Journal of Comparative Neurology*, 334(1), 19–46.
- Angelucci, A., Levitt, J. B., Walton, E. J. S., Hupe, J. M., Bullier, J., & Lund, J. S. (2002). Circuits for local and global signal integration in primary visual cortex. *Journal of Neuroscience*, 22(19), 8633–8646.
- Attwell, D., & Laughlin, S. B. (2001). An energy budget for signaling in the grey matter of the brain. *Journal of Cerebral Blood Flow and Metabolism*, 21, 1133–1145.
- Bandettini, P. A., Jesmanowicz, A., Wong, E. C., & Hyde, J. S. (1993). Processing strategies for time-course data sets in functional MRI of the human brain. *Magnetic Resonance in Medicine*, 30, 161–173.
- Boynton, G. M., Demb, J. B., Glover, G. H., & Heeger, D. J. (1999). Neuronal basis of contrast discrimination. *Vision Research*, 39, 257–269.
- Brainard, D. H. (1997). The psychophysics toolbox. *Spatial Vision*, 10, 433–436.
- Caesar, K., Thomsen, K., & Lauritzen, M. (2003). Dissociation of spikes, synaptic activity, and activity-dependent increments in rat cerebellar blood flow by tonic synaptic inhibition. *Proceedings of the National Academy of Sciences, USA*, 100(26), 16000–16005.
- Cauli, B., Tong, X. K., Rancillac, A., Serluca, N., Lambolez, B., Rossier, J., et al. (2004). Cortical GABA interneurons in neurovascular coupling: Relays for subcortical vasoactive pathways. *Journal of Neuroscience*, 24(41), 8940–8949.
- Cavanaugh, J. R., Bair, W., & Movshon, J. A. (2002). Selectivity and spatial distribution of signals from the receptive field surround of macaque V1 neurons. *Journal of Neurophysiology*, 88, 2547–2556.
- Chen, Z., Silva, A. C., Yang, J., & Shen, J. (2005). Elevated endogenous GABA level correlates with decreased fMRI signals in the rat brain during acute inhibition of GABA transaminase. *Journal of Neuroscience Research*, 79, 383–391.
- Das, A., & Gilbert, C. D. (1995). Long-range horizontal connections and their role in cortical reorganization revealed by optical recording of cat primary visual cortex. *Nature*, 375, 780–784.
- Devor, A., Hillman, E. M. C., Tian, P., Waeber, C., Teng, I. C., Ruvinskaya, L., et al. (2008). Stimulus-induced changes in blood flow and 2-deoxyglucose uptake dissociate in ipsilateral somatosensory cortex. *The Journal of Neuroscience*, 28(53), 14347–14357.
- Devor, A., Tian, P., Nishimura, N., Teng, I. C., Hillman, E. M. C., Narayanan, S. N., et al. (2007). Suppressed neuronal activity and concurrent arteriolar vasoconstriction may explain negative blood oxygenation level-dependent signal. *Journal of Neuroscience*, 27(16), 4452–4459.
- DeYoe, E. A., Carman, G. J., Bandettini, P., Glickman, S., Wieser, J., Cox, R., et al. (1996). Mapping striate and extrastriate visual areas in human cerebral cortex. *Proceedings of the National Academy of Science, USA*, 93, 2382–2386.
- Engel, S. A., Glover, G. H., & Wandell, B. A. (1997). Retinotopic organization in human visual cortex and the spatial precision of functional MRI. *Cerebral Cortex*, 7, 181–192.

- Grinvald, A., Lieke, E. E., Frostig, R. D., & Hildesheim, R. (1994). Cortical point-spread function and long-range lateral interactions revealed by real-time optical imaging of macaque monkey primary visual cortex. *Journal of Neuroscience*, *14*(5), 2545–2568.
- Hulvershorn, J., Bloy Lee, G., Leigh, J. S., & Elliott, M. A. (2005). Spatial sensitivity and temporal response of spin echo and gradient echo bold contrast at 3T using peak hemodynamic activation time. *NeuroImage*, *24*, 216–223.
- Hupe, J. M., James, A. C., Payne, B. R., Lomber, S. G., Girard, P., & Bullier, J. (1998). Cortical feedback improves discrimination between figure and background by V1, V2 and V3 neurons. *Nature*, *394*(6695), 784–787.
- Jenkinson, M., Bannister, P. R., Brady, J. M., & Smith, S. M. (2002). Improved optimization for the robust and accurate linear registration and motion correction of brain images. *NeuroImage*, *17*(2), 825–841.
- Kamitani, Y., & Tong, F. (2005). Decoding the visual and subjective contents of the human brain. *Nature Neuroscience*, *8*(5), 679–685.
- Kastner, S., De Weerd, P., Pinsk, M. A., Elizondo, M. I., Desimone, R., & Ungerleider, L. G. (2001). Modulation of sensory suppression: Implications for receptive field sizes in the human visual cortex. *Journal of Neurophysiology*, *86*, 1398–1411.
- Kay, K. N., Naselaris, T., Prenger, R. J., & Gallant, J. L. (2008). Identifying natural images from human brain activity. *Nature*, *452*, 352–355.
- Kinoshita, M., Gilbert, C. D., & Das, A. (2009). Optical imaging of contextual interactions in V1 of the behaving monkey. *Journal of Neurophysiology*, *102*, 1930–1944.
- Kriegeskorte, N., Cusack, R., & Bandettini, P. (2010). How does an fMRI voxel sample the neuronal activity pattern: Compact-kernel or complex spatiotemporal filter? *NeuroImage*, *49*(3), 1965–1976.
- Larsson, J. (2001). Imaging vision: Functional mapping of intermediate visual processes in man, PhD, Stockholm: Karolinska Institutet.
- Larsson, J., Landy, M. S., & Heeger, D. J. (2006). Orientation-selective adaptation to first- and second-order patterns in human visual cortex. *Journal of Neurophysiology*, *95*, 862–881.
- Lauritzen, M. (2001). Relationship of spikes, synaptic activity, and local changes of cerebral blood flow. *Journal of Cerebral Blood Flow and Metabolism*, *21*, 1367–1383.
- Li, J., & Iadecola, C. (1994). Nitric oxide and adenosine mediate vasodilation during functional activation in cerebellar cortex. *Neuropharmacology*, *33*(11), 1453–1461.
- Logothetis, N. K. (2003). The underpinnings of the BOLD functional magnetic resonance imaging signal. *Journal of Neuroscience*, *23*(10), 3963–3971.
- Mathiesen, C., Caesar, K., Akgören, N., & Lauritzen, M. (1998). Modification of activity-dependent increases of cerebral blood flow by excitatory synaptic activity and spikes in rat cerebellar cortex. *Journal of Physiology*, *512*(2), 555–566.
- Nestares, O., & Heeger, D. J. (2000). Robust multiresolution alignment of MRI brain volumes. *Magnetic Resonance in Medicine*, *43*, 705–715.
- Nie, F., & Wong-Riley, M. T. T. (1995). Double labeling of GABA and cytochrome oxidase in the macaque visual cortex: Quantitative EM analysis. *Journal of Comparative Neurology*, *356*, 115–131.
- Northoff, G., Walter, M., Schulte, R. F., Beck, J., Dydak, U., Henning, A., et al. (2007). GABA concentrations in the human anterior cingulate cortex predict negative BOLD responses in fMRI. *Nature Neuroscience*, *10*, 1515–1517.
- Nurminen, L., Kilpeläinen, M., Laurinen, P., & Vanni, S. (2009). Area summation in human visual system: Psychophysics, fMRI and modeling. *Journal of Neurophysiology*, *102*, 2900–2909.
- Ogawa, S., Menon, R. S., Tank, D. W., Kim, S. G., Merkle, H., Ellermann, J. M., et al. (1993). Functional brain mapping by blood oxygenation level-dependent contrast magnetic resonance imaging. *Biophysical Journal*, *64*, 803–812.
- Olman, C. A., Inati, S., & Heeger, D. J. (2007). The effect of large veins on spatial localization with GE BOLD at 3T: Displacement, not blurring. *NeuroImage*, *34*, 1126–1135.
- Parkes, L. M., Schwarzbach, J. V., Bouts, A. A., Deckers, R. R., Pullens, P., Kerskens, C. M., et al. (2005). Quantifying the spatial resolution of the gradient echo and spin echo BOLD response at 3 Tesla. *Magnetic Resonance in Medicine*, *54*, 1465–1472.
- Patel, A. B., de Graaf, R. A., Mason, G. F., Rothman, D. L., Shulman, R. G., & Behar, K. L. (2005). The contribution of GABA to glutamate/glutamine cycling and energy metabolism in the rat cortex in vivo. *Proceedings of the National Academy of Sciences, USA*, *102*(15), 5588–5593.
- Pelled, G., Bergstrom, D. A., Tierney, P. L., Conroy, R. S., Chuang, K. H., Yu, D., et al. (2009). Ipsilateral cortical fMRI responses after peripheral nerve damage in rats reflect increased interneuron activity. *Proceedings of the National Academy of Sciences, USA*, *106*(33), 14114–14119.
- Pelli, D. G. (1997). The VideoToolbox software for visual psychophysics: Transforming numbers into movies. *Spatial Vision*, *10*, 437–442.
- Petrov, Y., Carandini, M., & McKee, S. (2005). Two distinct mechanisms of suppression in human vision. *Journal of Neuroscience*, *25*(38), 8704–8707.
- Pihlaja, M., Henriksson, L., James, A. C., & Vanni, S. (2008). Quantitative multifocal fMRI shows active suppression in human V1. *Human Brain Mapping*, *29*, 1001–1014.
- Polat, U., Mizobe, K., Pettet, M. W., Kasamatsu, T., & Norcia, A. M. (1998). Collinear stimuli regulate visual responses depending on cell's contrast threshold. *Nature*, *391*, 580–584.
- Schwabe, L., Obermayer, K., Angelucci, A., & Bressloff, P. C. (2006). The role of feedback in shaping the extra-classical receptive field of cortical neurons: A recurrent network model. *Journal of Neuroscience*, *26*(36), 9117–9129.
- Sereno, M. I., Dale, A. M., Reppas, J. B., Kwong, K. K., Belliveau, J. W., Brady, T. J., et al. (1995). Borders of multiple visual areas in humans revealed by functional magnetic resonance imaging. *Science*, *268*, 889–893.
- Shmuel, A., Augath, M., Oeltermann, A., & Logothetis, N. K. (2006). Negative functional MRI response correlates with decreases in neuronal activity in monkey visual area V1. *Nature Neuroscience*, *9*(4), 569–577.
- Smith, S. M., Jenkinson, M., Woolrich, M. W., Beckmann, C. F., Behrens, T. E. J., Johansen-Berg, H., et al. (2004). Advances in functional and structural MR image analysis and implementation as FSL. *NeuroImage*, *23*, S208–S219.
- Sotero, R. C., & Trujillo-Barreto, N. J. (2007). Modelling the role of excitatory and inhibitory neuronal activity in the generation of the BOLD signal. *NeuroImage*, *35*, 149–165.
- Vaucher, E., Tong, X.-K., Cholet, N., Lantin, S., & Hamel, E. (2000). GABA neurons provide a rich input to microvessels but not nitric oxide neurons in the rat cerebral cortex: A means for direct regulation of local cerebral blood flow. *The Journal of Comparative Neurology*, *421*, 161–171.
- Williams, A. L., Singh, K. D., & Smith, A. T. (2003). Surround modulation measure with functional MRI in the human visual cortex. *Journal of Neurophysiology*, *89*, 525–533.
- Xing, J., & Heeger, D. J. (2000). Center-surround interactions in foveal and peripheral vision. *Vision Research*, *40*, 3065–3072.
- Zenger-Landolt, B., & Heeger, D. J. (2003). Response suppression in V1 agrees with psychophysics of surround masking. *Journal of Neuroscience*, *23*(17), 6884–6893.
- Zenger-Landolt, B., & Koch, C. (2001). Flanker effects in peripheral contrast discrimination – psychophysics and modeling. *Vision Research*, *41*, 3663–3675.
- Zipsper, K., Lamme, V. A., & Schiller, P. H. (1996). Contextual modulation in primary visual cortex. *Journal of Neuroscience*, *16*(22), 7376–7389.